



Expression and characterization of novel chimeric endolysin CHAPk-SH3bk against biofilm-forming methicillin-resistant *Staphylococcus aureus*

Manisha Behera^{a,b}, Gagandeep Singh^{c,d}, Ashutosh Vats^b, Parmanand^b, Mayank Roshan^b, Devika Gautam^b, Chanchal Rana^b, Rajesh Kumar Kesharwani^e, Sachinandan De^{b,*}, Soma M. Ghorai^{a,**}

^a Department of Zoology, Hindu College, University of Delhi, Delhi 110007, India

^b National Dairy Research Institute (NDRI), Animal Biotechnology Centre, Animal Genomics Lab, Karnal 132001, Haryana, India

^c Section of Microbiology, Central Ayurveda Research Institute, Jhansi, Uttar Pradesh, India

^d Kusuma School of Biological Sciences, Indian Institute of Technology, Delhi, India

^e Department of Computer Application, Nehru Gram Bharati (Deemed to be University), Prayagraj, India

ARTICLE INFO

Keywords:

Biofilm
MRSA
Bacteriophage endolysin
Chimeric endolysin
Antibacterial activity
Bacteriophage

ABSTRACT

The continuous evolution of antibiotic resistance in methicillin-resistant *Staphylococcus aureus* (MRSA) due to the misuse of antibiotics lays out the need for the development of new antimicrobials with higher activity and lower resistance. In this study, we have expressed novel chimeric endolysin CHAPk-SH3bk derived from LysK to investigate its antibacterial activity against planktonic and biofilm-forming MRSA. The molecular docking and MD simulation results identified critical amino acids (ASP47, ASP56, ARG71, and Gly74) of CHAPk domain responsible for its catalytic activity. Chimeric endolysin CHAPk-SH3bk showed an effective binding to peptidoglycan fragment using 14 hydrogen bonds. The in-vitro antibacterial assays displayed higher activity of CHAPk against planktonic MRSA with 2-log₁₀ reduction in 2 h. Both CHAPk and CHAPk-SH3bk displayed bactericidal activity against MRSA with ~4log₁₀ and ~3.5log₁₀ reduction in 24 h. Biofilm reduction activity displayed CHAPk-SH3bk reduced 33 % and 60 % of hospital-associated ATCC®BAA-44™ and bovine origin SA1 respectively. The CHAPk treatment reduced 47 % of the preformed biofilm formed by bovine-origin MRSA SA1. This study indicates an effective reduction of preformed MRSA biofilms of human and animal origin using novel chimeric construct CHAPk-SH3bk. Stating that the combination and shuffling of different domains of phage endolysin potentially increase its bacteriolytic effectiveness against MRSA.

1. Introduction

Staphylococcus aureus is a common Gram-positive bacterium with commensal as well as pathogenic relationships with humans [1]. As a commensal organism, it colonizes about 30 % of the human population's nasal cavities, followed by skin, armpits, and throat [2]. Pathogenic *S. aureus* causes skin and soft tissue infections, osteomyelitis, bacteremia, pneumonia, and endocarditis in humans [3]. The challenge to treat pathogenic *S. aureus* has escalated due to the emergence of antibiotic-resistant strains, notably methicillin-resistant *S. aureus* (MRSA). MRSA is resistant to almost all β-lactam antibiotics commercially available. The MRSA surfaced as hospital-associated (HA)-MRSA infections in the 1960s. Later it developed as community-associated (CA)-MRSA, and

livestock-associated (LA)-MRSA in the 1990s and 2003 respectively. The association of MRSA to various microbiomes represented it as a major concern under the one-health concept [4].

Since 1999, Indian hospitals have also been grappling with the threat of MRSA infections [5]. Numerous studies have reported MRSA infection exceeding 40 % during the year 2008–2009. A study conducted in a tertiary care Indian hospital in 2017 revealed a higher rate of HA-MRSA (65 %) than CA-MRSA (35 %) [5]. The incidence of *S. aureus* in HA-associated infections is elevated due to the pathogen's biofilm-forming ability, which allows it to adhere and form biofilm on medical equipment such as catheters, and prosthetic devices (Eyeglasses, hearing aids, pacemakers, orthopaedic shoes, braces, and bone plates). *Staphylococcal* biofilms are self-secreted extracellular polymeric matrices inhabiting

* Corresponding author at: AGL, Animal Biotechnology Centre, ICAR-National Dairy Research Institute, Karnal, HR, India.

** Corresponding author at: Department of Zoology, Hindu College, University of Delhi, India.

E-mail addresses: sachinandan@gmail.com (S. De), somamghorai@hindu.du.ac.in (S.M. Ghorai).

persist bacterial cells [6]. The biofilm matrix formed by *S. aureus* exhibits an increased antibiotic resistance compared to planktonic cells leading to chronic infections [7]. Biofilm formation inhibits the treatment of bacterial cells inside the biofilm matrix and increases the resistance to antibiotics in both humans and animals [8]. Likewise, MRSA associated with bovine mastitis infection inhabits mammary gland as persistent bacteria buried inside biofilm. The MRSA forming biofilm and those acting as persister cells precludes the action of antibiotics, restricting the use of antibiotics in veterinary hospitals and tertiary care units [9].

The high use of antibiotics in tertiary care units has led to the development of antibiotic-resistant strains like MRSA [10]. Therefore, the application of novel antimicrobials such as antimicrobial peptides, nanoparticles, phage therapy or bacteriophage endolysins is the need of the hour to control MRSA infection. The ability of bacteriophage endolysins to lyse bacterial cells from inside at the end of lytic life mark them as promising antibacterial agent [11]. These bacteriophage endolysins confer a higher degree of specificity towards pathogens without developing resistance against bacteria compared to other antimicrobials [12]. The application of modular endolysins on Gram-positive bacteria has been explored in various ways to inhibit or eradicate the growth of MRSA [13]. The bacteriophages infecting *S. aureus* commonly feature endolysins with a unique 3-domain architecture composed of one or two enzymatically active domains (EAD) (cysteine, histidine-dependent amidohydrolase/peptidase; CHAP at the N-terminus, *N*-acetylmuramoyl-L-alanine amidase at a central position) and one C-terminal cell wall binding domain (CBD) SH3-type [12]. Therefore, we hypothesized that randomly altering the domains of *Staphylococcal* endolysins could create a chimeric endolysin with enhanced lytic activity against biofilm-forming MRSA. The domain shuffling method could engineer the endolysin and enhance desirable properties, such as bacteriolytic activity, increased solubility, and broadened host range [14]. Endolysin LysK has been explored for its antibacterial activity in various combinations such as; LysK CHAP domain (amino acids 1–165) [15], CHAP (amino acids 38–164) - amidase construct (amino acids 210–334), [16] and LysK221–390 (with a deletion of amidase domain 222–343) construct [17]. Both the constructs CHAP-amidase and LysK221–390 have shown significant bacteriolytic activity against different MRSA strains. The SH3b domain of LysK has been examined in combination with EADs of other endolysins, revealing an enhancement in bacteriolytic activity against MRSA [18,19] This study is aimed to design and express a novel chimeric endolysin composed of endolysin LysK CHAPk domain and SH3b domain. The study proposes to investigate the antibacterial activity of novel chimeric endolysin CHAPk-SH3bk and compare its lytic activity to CHAPk against MRSA biofilm formation. Additionally, the study seeks to determine the significance of the presence of cell wall binding domain in augmenting the lytic activity against preformed biofilms.

2. Materials and methods

2.1. Bacterial strains

The MRSA strain used in this study includes *S. aureus* (ATCC® BAA-44™) HiMedia, India. Other four MRSA isolates used in this study were isolated from the bovine clinical-mastitis infected milk samples as described earlier in Roshan et al. 2022 [20]. Briefly, the infected milk samples were streaked on mannitol salt agar (MSA) plates (GMH118, HiMedia, India) supplemented with 4 µg/ml oxacillin. The plates were incubated overnight at 37 °C for the growth of yellow-colored *S. aureus* colonies. The suspected *S. aureus* colonies resistant to oxacillin were subjected to DNA isolation. The molecular detection of methicillin resistance gene *mecA* and virulence genes (*coa*, and *nuc*) was performed using monoplex PCR. The primer details are mentioned in table S1. The mannitol-fermenting yellow-colored colonies phenotypically resistant to oxacillin and positive for all three genes (*mecA*, *coa*, and *nuc*) were

confirmed as MRSA and stored in 80 % glycerol for further testing. The *E. coli* strains used in this study includes *E. coli* (DH5α) and *E. coli* BL21 (DE3) for DNA cloning and protein expression, respectively.

2.2. Bioinformatics analysis of endolysin LysK

The sequence of endolysin LysK was retrieved from the NCBI database (<https://www.ncbi.nlm.nih.gov/>) [GenBank: AY176327]. The functional domain analysis was carried out using SMART (<http://smart.embl-heidelberg.de/>) and InterPro (<https://www.ebi.ac.uk/interpro/search/sequence/>). The ProtParam (<https://web.expasy.org/protparam/>) and SAS (<https://www.ebi.ac.uk/thornton-srv/databases/sas/>) servers were used to investigate the primary and secondary structure respectively, for CHAP and SH3b domain. The ConSurf (https://consurf.tau.ac.il/consurf_index.php) was used to estimate the evolutionary lineage and critical amino acid binding sites of CHAP and SH3b. The CHAPk-SH3bk was constructed by fusing the CHAP domain (amino acid 1–165) with the SH3b domain (amino acid 409–487) using the GS linker (GSGSGS). The stability and primary structure of the construct was analyzed using ProtParam and the 3D structure of the chimeric endolysin was modeled using IntFOLD (<https://www.reading.ac.uk/bioinf/IntFOLD/>).

2.3. Protein modeling and molecular docking of CHAP, SH3b, and CHAPk-SH3bk

The amino acid sequence of the CHAP and SH3b domains were retrieved and subjected to homology modeling using the SWISS-MODEL (<https://swissmodel.expasy.org/interactive>) server. The template for each domain was selected based on sequence identity and coverage (Table 1). The selected models of CHAP, SH3b, and CHAPk-SH3bk structural constraints were verified using a Ramachandran plot generated using PROCHECK (<https://servicesn.mbi.ucla.edu/PROCHECK/>) and MolProbity (<http://molprobity.biochem.duke.edu/>). The CHAP domain was docked against ligand Glycyl-D-Alanine and Chitin with PubChem ID 11966077 and 6857375, respectively. The SH3b domain was docked with Pentaglycine (PubChem ID 81537) and D-Ribitol-5-phosphate (PubChem ID 151104). The CHAPk-SH3bk was docked against the peptidoglycan (PG) fragment and modeled using the SMILES code provided in Mitkowski et al. 2019 [21]. The protein-ligand docking was performed using Autodock4.2 (<https://autodock.scripps.edu/download-autodock4/>). Docking results were analyzed using PyMOL (<https://pymol.org/2/>) and Ligplot (<https://www.ebi.ac.uk/thornton-srv/software/LigPlus/>).

2.4. Molecular dynamics simulations

The MD simulations were carried out to understand the dynamics of protein-ligand interaction. The lowest energy docked complexes of CHAP-Chitin, CHAP-Glycyl-D-Alanine, SH3b-Pentaglycine, SH3b-D-Ribitol-5-phosphate and CHAPk-SH3bk-PG fragment were selected for MD simulation process. All the simulations were carried out using GROMACS 5.1.5 [22]. The systems were prepared as previously described by Singh et al. 2022 [23]. Briefly, the AMBER99SB forcefield was used for preparing protein topology and the AnteChamber package from AmberTools21 was used for generating ligand parameters (AM1-BCC charges) with the GAFF2 forcefield. The complexes were centered in cubic boxes with an edge distance of 10 Å, filled with TIP3P water molecules, and neutralized the system with 0.15 M NaCl. The systems were energy minimized using the steepest descent algorithm with a step size of 0.01 nm. Subsequent equilibrations were done at 310.15 K and 1 atm for 1 ns; each using a modified Berendsen thermostat and Parinello-Rahman barostat, respectively. The production MD was run for 100 ns each, with a time step of 2f, and frames were stored at an interval of 10 ps. The trajectories were analyzed using standard GROMACS tools and PyMol (<https://pymol.org/2/>). The data for RMSD, RMSF, the radius of

Table 1

List and details of templates selected for molecular docking of CHAPk, SH3bk, and CHAPk-SH3bk.

S. No	Domain	Template	Sequence identity	Coverage	QMEAN	% Residue in most favored regions of Ramachandran plot (PROCHECK)	% Residue in most favored regions of Ramachandran plot (MolProbity)
1.	CHAP	4olk.1	98.75 %	1.00	0.94 ± 0.07	87.2 %	96.91 %
2.	SH3b	5o1q.1	100 %	1.00	0.72 ± 0.11	88.8 %	92.31 %
3.	CHAPk-SH3bk					88.4 %	92.16 %

gyration, and hydrogen bond interactions were acquired using standard GROMACS tools and their corresponding plots were generated using the GNUPLOT5.4 plotting tool (<http://www.gnuplot.info/>).

2.5. Construction of chimeric CHAPk-SH3bk, expression and purification

The *E. coli*-optimized gene coding sequences of CHAPk and CHAPk-SH3bk were synthesized by GenScript, USA. The sequences were inserted into the *EcoRV*-*EcoRV* cloning site of the pUC57 plasmid. The gene sequences in pUC57 amplified using primers having BamHI and *XhoI* restriction enzyme sites were subcloned into a pET-22b(+) expression vector including a C-terminal 6 × His-tag and pelB signal sequence. The double digestion of amplified gene fragments and pET-22b(+) vector was performed using restriction enzymes BamHI (Thermo Scientific™ FastDigest BamHI, FD0054) and *XhoI* (Thermo Scientific™ FastDigest *XhoI*, FD0695), which was followed by T4 DNA ligation using T4 DNA ligase (Thermo Scientific™ T4 DNA Ligase, EL0011). The cloning was confirmed by PCR amplification using vector-specific T7 promoter, terminator primers, and insert-specific primers. The CHAPk and CHAPk-SH3bk cloned in the pET-22b(+) vector were transformed into *E. coli* BL21 (DE3) competent cells at 37 °C in LB (Luria Bertani) medium (M1245, HiMedia, India) containing 50 mg/ml of ampicillin. The cultures were grown for 2–3 h in LB broth. The culture with O.D_{600nm} ~ 1.0 was induced using IPTG (Thermo Scientific™ IPTG, dioxane-free, R0392), added to a final concentration of 1 mM, and further incubated for 16–18 h at 16 °C. The bacterial cell pellet was harvested and processed for the cold osmotic shock to prepare periplasmic extract carrying expressed protein. Protein expression was determined by SDS-PAGE analysis of periplasmic fraction followed by staining with Coomassie blue. Recombinant proteins were purified through Ni-IDA affinity chromatography using G-His protein purification kit (GDH01A, GCC BIOTECH (INDIA) PVT. LTD.) as per the manufacturer's instructions. Purified proteins were buffer exchanged and concentrated with the low salt buffer (10 mM Tris-HCl, 150 mM NaCl, 1 % glycerol; pH 7.5). The purified proteins were quantified using the Bradford assay. The purified proteins were analyzed using SDS-PAGE (10 %) followed by western blot using 6×-His-Tag Antibody (Invitrogen 6×-His Tag Monoclonal Antibody (HIS.H8), MA1–21315).

2.6. Zymogram analysis of CHAPk and CHAPk-SH3bk

The Zymogram assay was performed to check the bacteriolytic activity of CHAPk and CHAPk-SH3bk as previously described with slight modifications [24]. Briefly, the polyacrylamide gel of 12 % was prepared containing 0.2 % of autoclaved *S. aureus* (ATCC® BAA-44™). 5 µg and 10 µg of purified CHAPk and CHAPk-SH3bk were loaded along with a protein marker (Pierce™ Prestained Protein MW Marker, 26,612). After the SDS-PAGE run was complete, the gel was soaked in distilled water for 30 min to remove SDS followed by overnight incubation at 37 °C in renaturation buffer (50 mM Tris-HCl, pH 8.0, 1 % Triton X-100). The lytic areas of endolysin were detected by staining the gel with 0.1 % methylene blue in 0.01 % KOH and subsequently de-staining with distilled water.

2.7. Diffusion lysis assay of CHAPk and CHAPk-SH3bk

The Diffusion lysis assay was carried out as previously described with little modifications [25]. Briefly, exponentially growing cells of *S. aureus* (ATCC® BAA-44™) were harvested and washed twice with 1 × PBS (pH 7.5). The pellet was resuspended in agar powder (7.5 g/l) and autoclaved. The agar mixture was poured into a 90 mm petri dish. After solidification, two wells per plate were created diametrically opposite. The 50 µg of CHAPk and CHAPk-SH3bk were added to one well in each plate and 50 µl low salt buffer in the second well as the negative control. The plates were incubated overnight at 37 °C, and diffusion was evaluated by observing a clear zone around each well.

2.8. Bactericidal activity assay of CHAPk and CHAPk-SH3bk

The bactericidal activity of CHAPk and CHAPk-SH3bk was assessed using the CFU reduction assay [26]. Briefly, an overnight culture of *S. aureus* (ATCC® BAA-44™) was reinoculated in Brain Heart Infusion (BHI) broth (SRL, 87864, India) for ~3 h to obtain 1 × 10⁸ cells/ml. 100 µl (1 × 10⁷ cells) were treated with purified protein at specified concentrations (0.015 µg/µl, 0.05 µg/µl, 0.1 µg/µl, 0.2 µg/µl) in 100 µl volume and incubated at 37 °C, at 200 rpm for 2 h. To analyze endolysin's bacteriolytic activity, the residual viable bacterial cells (colony forming units; CFUs) were enumerated by serial dilution and plating on LB agar plates.

2.9. Time-kill curve study of CHAPk and CHAPk-SH3bk

To study the time-kill kinetics; overnight culture of *S. aureus* (ATCC® BAA-44™) was reinoculated in 5 ml BHI broth for 2–3 h to obtain 1 × 10⁸ cells/ml. The bacterial cells were harvested and washed twice with 1 × PBS (pH 7.5). The cell pellet was resuspended in 5 ml of 1 × PBS to a final density of 10⁷ CFU/ml. The 0.02 µg/µl of CHAPk and CHAPk-SH3bk in PBS with a volume of 50 µl was added to 450 µl of the cell suspension and incubated at 37 °C, at 200 rpm. To count initial CFU/ml at 0 h, 50 µl of aliquot was taken followed by collecting aliquots at respective time points (2, 4, 8, and 24 h) and cultures were diluted by a factor of 1/4 × 10⁻⁶, from which 100 µl samples were spread onto the LB agar plate. Colony forming units (CFUs) were calculated after overnight incubation at 37 °C.

2.10. Characterization of endolysin CHAPk-SH3bk

The thermal stability of endolysin CHAPk-SH3bk was tested using the CFU reduction assay. 0.05 µg/µl of CHAPk-SH3bk was incubated at different temperatures (4 °C, 20 °C, 37 °C, 50 °C, and 70 °C) for 30 min and suspended in 1 × PBS (pH 7.5). 50 µl of differently treated CHAPk-SH3bk is mixed with 50 µl (with a final density of ~10⁶CFU/ml) bacterial solution and incubated further for 30 min at 37 °C. The negative control contained 50 µl bacterial solution and 50 µl PBS without any temperature treatment. The bacteriolytic activity of CHAPk-SH3bk at different temperatures was analyzed by counting the residual viable bacterial cells (colony-forming units; CFUs) using serial dilution and plating.

To evaluate the effect of pH on the lytic activity, CHAPk-SH3bk (0.05 µg/µl) was added to *S. aureus* (ATCC® BAA-44™) cells suspended in 50 mM Tris-HCl (pH 4, 6, 8, 10 and 12). The thoroughly mixed reaction mixtures were incubated at 37 °C for 30 min, and OD measured at 600 nm. The relative lytic activity was calculated using the following equation [27]:

$$\text{lytic activity (\%)} = 100 \times (\text{OD}_{600\text{nm}} \text{ of control without enzyme} - \text{OD}_{600\text{nm}} \text{ of the reaction mixture with endolysin}) / \text{OD}_{600\text{nm}} \text{ of control without enzyme}$$

2.11. Biofilm reduction assay of CHAPk and CHAPk-SH3bk

The biofilm reduction assay was performed as previously described with some modifications [28]. Briefly, hospital-associated *S. aureus* (ATCC® BAA-44™) and four other MRSA strains (SA1, SA2, SA3, and SA4) isolated from bovine mastitis samples were grown in Tryptone Soya Broth (TSB) (LQ009A, Himedia, India) supplemented with 0.25 % D- (+) -glucose (G8644, Sigma) and kept for overnight incubation at 37 °C. These were further diluted (1:50) in TSB with 0.25 % glucose to obtain O-D ~ 0.1 at 600 nm. A volume of 200 µl of diluted culture was added to a 96-well tissue culture plate and incubated for 24-h at 37 °C. After incubation supernatant was aspirated out and washed with 200 µl PBS twice. A total volume of 200 µl is added to each well, where the biofilm-containing wells were treated with 0.05 µg/µl of CHAPk and CHAPk-SH3bk suspended in TSB with 0.25 % glucose and controls contained only 200 µl of TSB with 0.25 % glucose followed by incubation for 18-h at 37 °C. After incubation, the wells were washed with PBS and dried at 37 °C for 15 min. The biomass attached to the wells was determined by staining wells with 0.5 % w/v crystal violet (15 min) followed by washing with autoclaved water and solubilization in 33 % acetic acid; the final solution obtained was measured at OD_{570nm}.

2.12. Confocal laser scanning microscopy (CLSM)

The biofilms were grown on 12 × 12 mm² glass coverslips in a 12-well plate for confocal microscopy. Coverslips were inoculated with 200 µl of overnight *S. aureus* culture diluted to obtain O-D ~ 0.1 at 600 nm in 3 ml TSB with 0.25 % glucose and incubated for 24-h at 37 °C. After washing the biofilms twice with 1 × PBS, they were treated with 0.05 µg/µl of CHAPk and CHAPk-SH3bk suspended in TSB with 0.25 % glucose. The controls were suspended in TSB with 0.25 % glucose followed by incubation for 18-h at 37 °C. After treatment, biofilms were prepared for imaging as described previously [29]. Briefly, biofilms were washed with 1 × PBS and fixed with 2.5 % glutaraldehyde (4 °C, 1 h). The biofilms were washed again and stained with 4',6-Diamidino-2-phenylindole dihydrochloride (DAPI) (D8417-1MG, Sigma) according to the manufacturer's instructions. The stained biofilms were analyzed at 100× followed by z-stack scanning using CLSM (Leica TCS SP8, AOBs-Acousto Optical Beam Splitter based, Germany). Three-dimensional projections of the biofilms were analyzed using ImageJ [30] and the biomass, maximum thickness, and volume of microcolonies at the substratum were analyzed using COMSTAT software [31].

2.13. Scanning electron microscope (SEM)

For SEM analysis, biofilms were grown on 12 × 12 mm² glass coverslips in a 12-well plate as described above. After an 18-h treatment of 0.05 µg/µl of CHAPk and CHAPk-SH3bk suspended in TSB with 0.25 % glucose, biofilms were rinsed with 1 × PBS. The biofilms were then fixed

in 2.5 % glutaraldehyde solution prepared in 1 × PBS of pH 7.4 (4 °C, 20 h), followed by washing with 1 × PBS. Biofilms were dehydrated using a series of ethanol (30 %, 50 %, 75 %, 90 %, and 100 %) for 5 min in each solution. Biofilms were dried by the quorum critical point dryer, coated with chromium, and imaged using FESEM (TESCAN CLARA, TESCAN, Czech Republic).

2.14. Statistical analysis

All experiments were performed in triplicates. Statistical analysis and graphs were generated using GraphPad Prism 8.0 (GraphPad Software, USA). Results are shown as mean ± standard deviation of the mean. Statistical significance was analyzed using two-way ANOVA and Tukey's multiple comparisons tests. *P*-values of <0.05 were considered statistically significant.

3. Results

3.1. Sequence and domain analysis of LysK

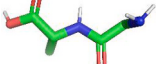
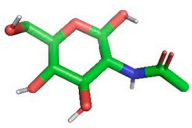
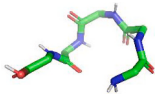
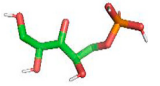
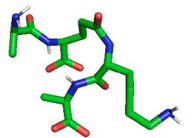
The Endolysin LysK identified from the genome sequence of *Staphylococcus* phage K (AY176327.1: 27072-29435) is a 54 kDa protein encoded by two open reading frames separated by an intron. The functional domain analysis using SMART and InterPro revealed LysK with a modular structure comprising CHAP domain, Amidase-2 domain, and SH3b domain (Fig. S1). The CHAPk, SH3bk, and CHAPk-SH3bk were characterized using ProtParam and considered as stable protein with their instability index at 36.44, 34.92, and 35.90 respectively; (the index below 40 means that the protein is stable). The secondary structure analysis revealed two alpha-helices, one 3₁₀-helix, and six beta-strands in CHAPk. The two alpha helices located at the N-terminal form a long loop whose base forms the catalytic site. This catalytic site was formed by the hydrophobic groove comprising amino acids CYS54, HIS117, and GLU134. Also, the conserved amino acids and the dynamics evolutionary conserved residues of ConSurf results demonstrated that CYS54, HIS117, and GLU134 amino acids are highly conserved in the CHAP domain (Fig. S2). The SH3bk domain of the LysK endolysin was found to be composed of nine beta-strands, which play a major role in *S. aureus* cell wall binding. The ConSurf results also indicated the conservation of amino acids in the beta sheets of SH3b domains and is an essential requirement to bind the bacterial peptidoglycan layer. The 3D structure of CHAPk-SH3bk was modeled using IntFOLD and is represented in Fig. S3.

3.2. Molecular docking analysis

The SWISS-MODEL modeled CHAPk, SH3bk domain, and IntFOLD modeled CHAPk-SH3bk were analyzed for the Ramachandran plot (Table 1). The Ramachandran plots and values indicated that 96.91 %, 92.31 %, and 92.16 % of residues were present in favored regions (Fig. S4). The modeled structures were docked with respective ligands (Table 2) using Autodock4.2. The best mode selected for each protein-ligand pair corresponds to the best binding affinity across 10 runs. The binding affinity and interacting amino acids of each domain are represented in Table 2. The common amino acid residues of the CHAPk domain interacting with Glycyl-D-Alanine and Chitin are ASP56 and ARG71, respectively (Fig. 1 a, b). The SH3bk domain docked with Pentaglycine displayed hydrogen bond interactions with amino acids ASN15, GLU62, ASN75, ARG81, and TYR83 (Fig. 1c). The ligand D-

Table 2

Result of molecular docking between CHAPk, SH3bk, and CHAPk-SH3bk with their respective ligands.

S. No	Endolysin LysK domain	Ligands	Ligand structure	Affinity (Kcal/mol)	No. of H-bond interactions	Interacting amino acid residues
1.	CHAPk	Glycyl-D-Alanine		-5.1	3	ASP47, ASP56, ARG71
2.	CHAPk	Chitin		-6.0	3	ASP56, ARG71, GLY74
3.	SH3bk	Pentaglycine		-5.0	5	ASN15, GLU62, ASN75, ARG81, TYR83
4.	SH3bk	D-Ribitol-5-phosphate		-4.3	4	TRP12, LYS22, ARG87, GLN96
5.	CHAPk-SH3bk	peptidoglycan fragment		-5.8	5	ASP47, ASP56, THR59, ARG71, GLY74

Ribitol-5-phosphate showed interactions with some critical amino acids of the SH3b domain like TRP12, LYS22, and ARG87 (Fig. 1d). The CHAPk-SH3bk bound peptidoglycan-fragment with binding affinity -5.8 kcal/mol formed hydrogen bond with amino acids ASP47, ASP56, THR59, ARG71, and GLY74 (Fig. 1e). This shows that CHAPk domain retains its interaction with peptidoglycan fragment even in the presence of cell wall binding domain SH3bk.

3.3. MD simulation analysis

The MD simulation study was carried out to assess the stability of CHAPk, SH3bk, and CHAPk-SH3bk with ligands including Glycyl-D-Alanine, Chitin, pentaglycine, D-Ribitol-5-phosphate, and PG fragment. The trajectory of Root Mean Square Deviation (RMSD) is used to measure the overall dynamics, stability, and convergence of the system. The RMSD trajectories of the CHAPk domain and in complex with Glycyl-D-Alanine were stable that indicated that CHAPk domain is stable during most of the run except between 40 and 60 ns and the last 10 ns of the run. As observed in the Fig. 2a, the ligand (Glycyl-D-Alanine) RMSD did not show value more than that of the CHAPk domain implying that it does not diffuse away from the catalytic site. Whereas, as compared to Glycyl-D-Alanine, ligand chitin was much more stable alone; as well as in complex with CHAPk domain. Only fluctuation was observed with an increase in RMSD after 60 ns till 100 ns of the run time (Fig. 2b). The RMSD of the CHAPk-Glycyl-D-Alanine complex and CHAPk-Chitin complex can be observed to have increased by ~ 0.07 nm from the CHAPk domain. This increase in RMSD can be attributed to the binding of the ligands to the catalytic sites of the CHAPk domain and forming hydrogen bonds. The RMSD plot of SH3bk ligands pentaglycine and D-Ribitol-5-phosphate display that the latter is much stable in the system. Also, if we compare the RMSD trajectory of the pentaglycine and D-Ribitol-5-phosphate in complex with SH3bk, with pentaglycine; SH3b was stable only for the last 40 ns (Fig. 2c). While with D-Ribitol-5-phosphate, SH3bk was stable during most of the run, except for the first

10 ns and between 35 and 40 ns (Fig. 2d). As compared to RMSD of SH3bk alone, in complex with ligands, an increase of ~ 1 nm was observed which indicates the interaction of ligands with SH3bk domain. The RMSD trajectory of protein CHAPk-SH3bk in complex with PG-fragment showed stability from 40 to 100 ns run time, with a fluctuation around 80 ns (Fig. 2e). The RMSD of the complex can be observed to have increased by ~ 0.05 nm from the protein, which might be the result of mobility in protein due to ligand binding. The results displayed interaction of CHAPk, SH3bk, and CHAPk-SH3bk with respective ligands is stable with a slight increase in RMSD indicating catalytic activity.

3.3.1. Root mean square fluctuation (RMSF)

RMSF of CHAPk, SH3bk, and CHAPk-SH3bk was calculated to observe the effect of ligand binding on the flexibility of each residue. The RMSF value of the CHAPk- Glycyl-D-Alanine complex lies between 0.04 nm–0.22 nm (Fig. S5a); while that of the CHAPk- Chitin complex lies between 0.04 nm–0.3 nm (Fig. S5b). The average RMSF in both CHAPk complexes is 0.1 nm. The RMSF graph displays more fluctuation in the N-terminal as compared to the C-terminal with violent fluctuations observed between amino acid residue 20–40 and 40–60 indicating the role of amino acids ASP47, ASP56, ARG71, and GLY74 in ligand binding. The catalytic residue CYS54 shows fluctuation in RMSF of 0.18 nm in the CHAPk- Glycyl-D-Alanine complex while 0.3 nm in the CHAPk – Chitin complex. The catalytic residues HIS117 and GLU134 of the CHAPk catalytic triad displayed RMSF of 0.1 nm in both complexes. This indicates the interaction of catalytic triad CYS54, HIS117, and GLU134 with the Glycyl-D-Alanine region of the endopeptide bond present in the *S. aureus* peptidoglycan layer. The RMSF graph of the SH3bk-Pentaglycine complex (Fig. S5c) does not show much fluctuation with a value of the RMSF between 0.09 nm – 0.75 nm. The average RMSF observed was ~ 0.1 nm. The violent fluctuation observed was between the C-terminal residues 75–80 (0.2 nm). The low flexibility of the SH3bk domain in complex with pentaglycine may be attributed to the

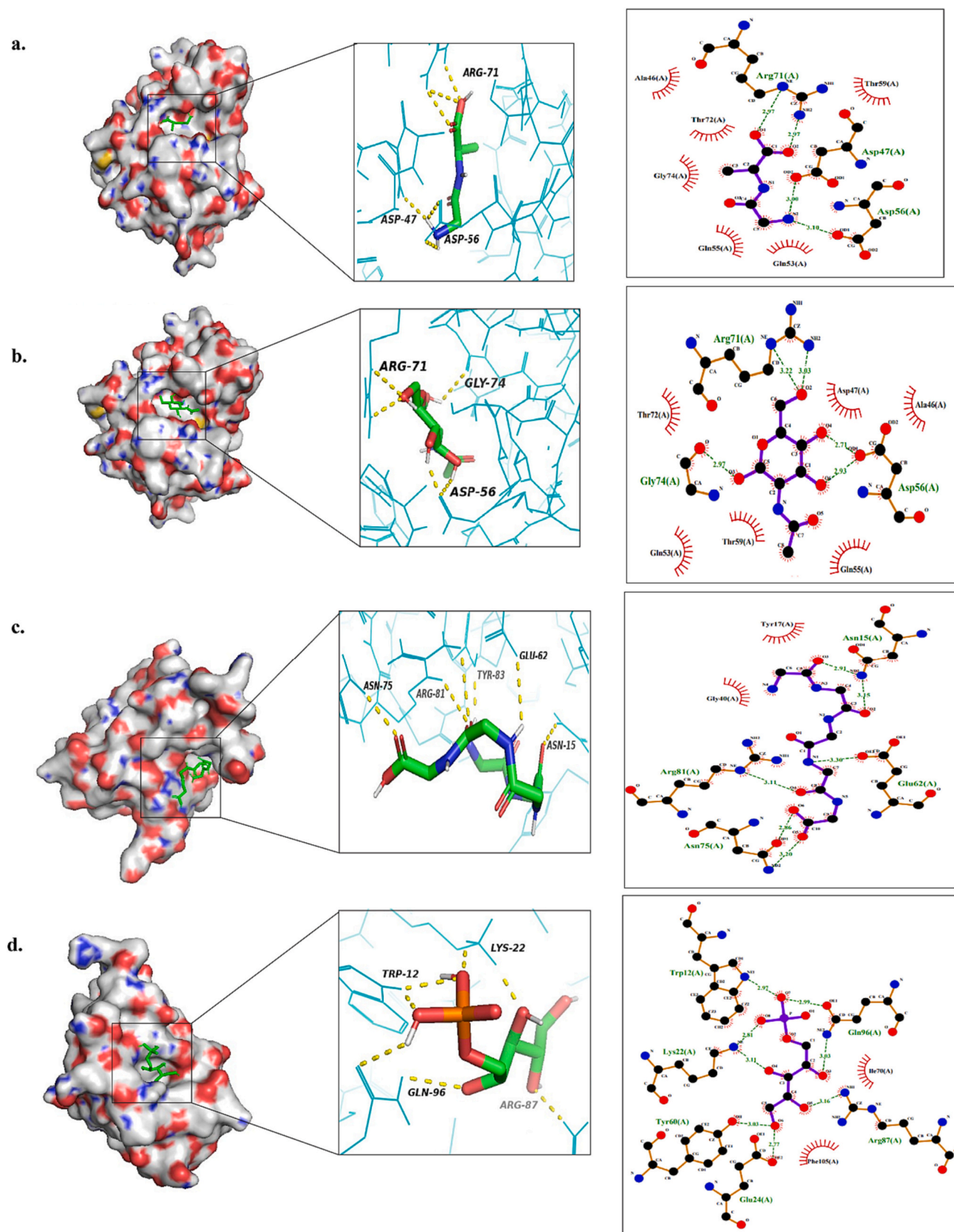


Fig. 1. Molecular docking results: Three dimensional structures of CHAPk, SH3bk and CHAPk-SH3bk showing the binding sites (left), and main residues involved in the ligand-protein interactions (right) followed by 2-D plot hydrogen bond interactions (a) CHAPk- Glycyl-D-Alanine (b) CHAPk- Chitin, (c) SH3bk- Pentaglycine, (d) D-Ribitol-5-phosphate, (e) CHAPk-SH3bk- PG fragment.

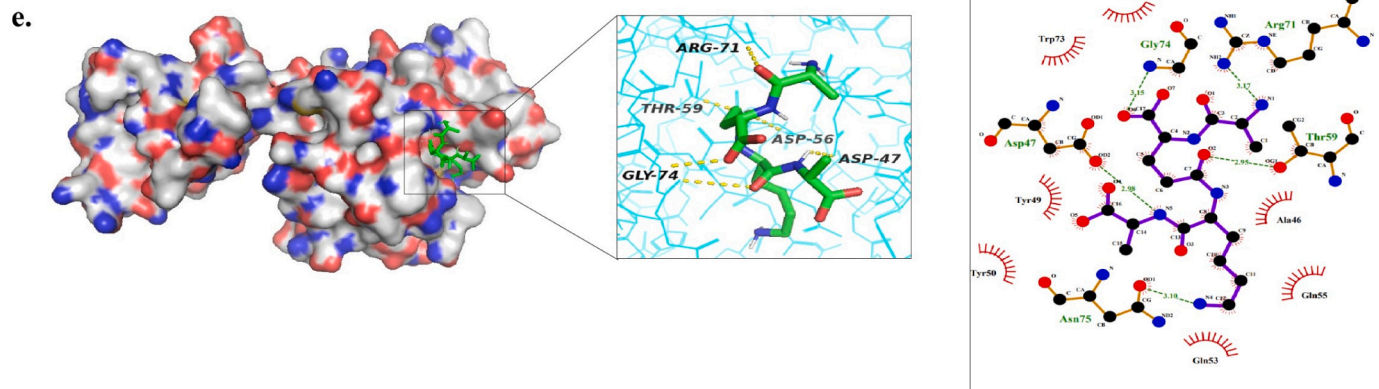


Fig. 1. (continued).

secondary structure of SH3bk composed of 9 β -sheets and compact binding of the SH3bk domain to the pentaglycine region of *S. aureus* peptidoglycan layer. In contradiction to this, the RMSF of SH3bk-D-Ribitol-5-phosphate complex (Fig. S5d) displayed an RMSF value between 0.05 nm – 0.44 nm with violent fluctuations in the C-terminal. Residue ASN45 displayed RMSF of 0.19 nm, residues ILE65, and ASN80 showed RMSF of 0.18 nm, and amino acid residue GLN90 displayed the most violent fluctuation at 0.24 nm. The high RMSF of SH3bk with D-Ribitol-5-phosphate indicates high mobility of residues when the SH3bk domain interacts with the teichoic acid component of *S. aureus* cell wall. The RMSF value of CHAPk-SH3bk in complex with PG-fragment was between 0.1 nm–0.6 nm with an average of 0.35 nm (Fig. S5e). The RMSF graph displayed more fluctuation in the C-terminal as compared to N-terminal. The residues (amino acid 47–74) of the CHAPk domain in interaction with PG-fragment displayed RMSF of \sim 0.3 nm, signifying their role in ligand binding and catalytic activity. The SH3bk domain in CHAPk-SH3bk displayed more fluctuation in the C-terminal with amino acid 230–240 displaying RMSF of 0.5–0.6 nm. The results displayed that the CHAPk domain is much more compact and stable in the presence of the SH3bk domain.

3.3.2. Radius of gyration

The radius of gyration (Rg) determines the compactness of the protein structure in the dynamic system. The less the value of Rg, the more stable and compact the protein in a complex with the ligand. The Rg of the CHAPk domain in complex with Glycyl-D-Alanine and Chitin displayed a range of 1.46 nm – 1.49 nm (Fig. S6a, S6b), with the average Rg of 1.475 nm. The CHAPk- Glycyl-D-Alanine complex displayed constant Rg after the first 20 ns and the CHAPk- Chitin complex Rg remained constant with a dip after 50 ns. This confirms that the CHAP protein is compact and stable. The Rg of SH3bk domain in complex with Pentaglycine and D-Ribitol-5-phosphate displayed an average of 1.32 nm (Fig. S6c, S6d). The stability with the pentaglycine ligand is attained in the last 40 ns, while with D-Ribitol-5-phosphate, it was stable throughout the run after the first 10 ns. This signifies SH3bk domain was much more stable in complex with D-Ribitol-5-phosphate as compared to Pentaglycine. The CHAPk-SH3bk-PG fragment complex displayed Rg range of 1.8 nm–2.19 nm, with an average of 1.99 nm (Fig. S6e). The CHAPk-SH3bk-PG fragment complex was not stable only during 60–80 ns, but was constant till 60 ns and for the last 20 ns. The results confirm the stability of CHAPk-SH3bk in a complex with peptidoglycan fragment with compact folding throughout most of the run time.

3.3.3. Hydrogen bond analysis

To understand the stability of complexes during MD simulation, the number of hydrogen bonds formed between protein and ligand were analyzed. The CHAPk in complex with Glycyl-D-Alanine and chitin

(Fig. S7a, b) showed a minimum of 3 hydrogen bonds stabilizing the complex, though a maximum number of 6 hydrogen bonds was observed. The Pentaglycine and D-Ribitol-5-phosphate formed a minimum of 2 hydrogen bonds throughout the run with the SH3bk domain (Fig. S7c). The interaction between the SH3b domain and D-Ribitol-5-phosphate displayed a minimum of 2 hydrogen bonds throughout the run (Fig. S7d). The ligand peptidoglycan-fragment made a maximum of 14 hydrogen bonds with CHAPk-SH3bk construct with a minimum of 8 hydrogen bonds that was maintained throughout the run (Fig. S7e). The results displayed interaction of CHAPk-SH3bk with bonds of *S. aureus* peptidoglycan layer is much more effective as compared to the CHAPk or SH3bk domain alone.

3.4. Purification, SDS-PAGE, and zymogram analysis

The chimeric endolysin CHAPk-SH3bk and CHAPk cloned in pET-22b(+) were expressed productively using 1 mM IPTG, followed by immobilized metal ion affinity chromatography. The SDS-PAGE and western blot analysis of isolated proteins CHAPk-SH3bk and CHAPk displayed discrete bands at their predicted molecular weight of 28 kDa and 22.6 kDa, respectively (Fig. 3a). A zymogram gel was run to check the lytic activity of purified proteins, and the appearance of a clear band at the predicted molecular weight for CHAPk-SH3bk and CHAPk show a strong PG hydrolysis activity (Fig. 3b).

3.5. Antibacterial assay against MRSA

The antibacterial activity of the CHAPk-SH3bk and CHAPk was first compared using diffusion lysis assay and bactericidal assay. The endolysin CHAPk-SH3bk showed a small region of clearance as compared to CHAPk which was found to form clear, round, significant halos in the agar plate containing heat-inactivated *S. aureus* (Fig. 4a). Further, to verify the bactericidal activity of endolysin CHAPk-SH3bk and CHAPk, *S. aureus* (ATCC® BAA-44™) was challenged with different concentrations of purified proteins. The results showed that the 2-h treatment of 0.2 μ g/ μ l CHAPk caused a 2- \log_{10} reduction in colony-forming units (CFU/ml) when the initial concentration was 10^8 CFU/ml as compared to 0.2 μ g/ μ l CHAPk-SH3bk, that could reduce CFU/ml by only 1- \log_{10} unit (Fig. 4b). The time-dependent killing assay for CHAPk-SH3bk and CHAPk were performed using *S. aureus* (ATCC® BAA-44™) cultures treated with 0.02 μ g/ μ l of each lytic protein. Incidentally, both CHAPk-SH3bk and CHAPk displayed similar reduction in the viable cell count with time. After 4-h of incubation, a reduction of \sim 0.7- \log_{10} unit was observed, followed by a 1- \log_{10} unit reduction after 8-h of incubation. After 24-h of incubation, 0.02 μ g/ μ l CHAPk displayed \sim 4- \log_{10} reduction in CFU/ml compared to CHAPk-SH3bk, which displayed a reduction of \sim 3.5- \log_{10} in CFU/ml. The results confirmed bactericidal activity

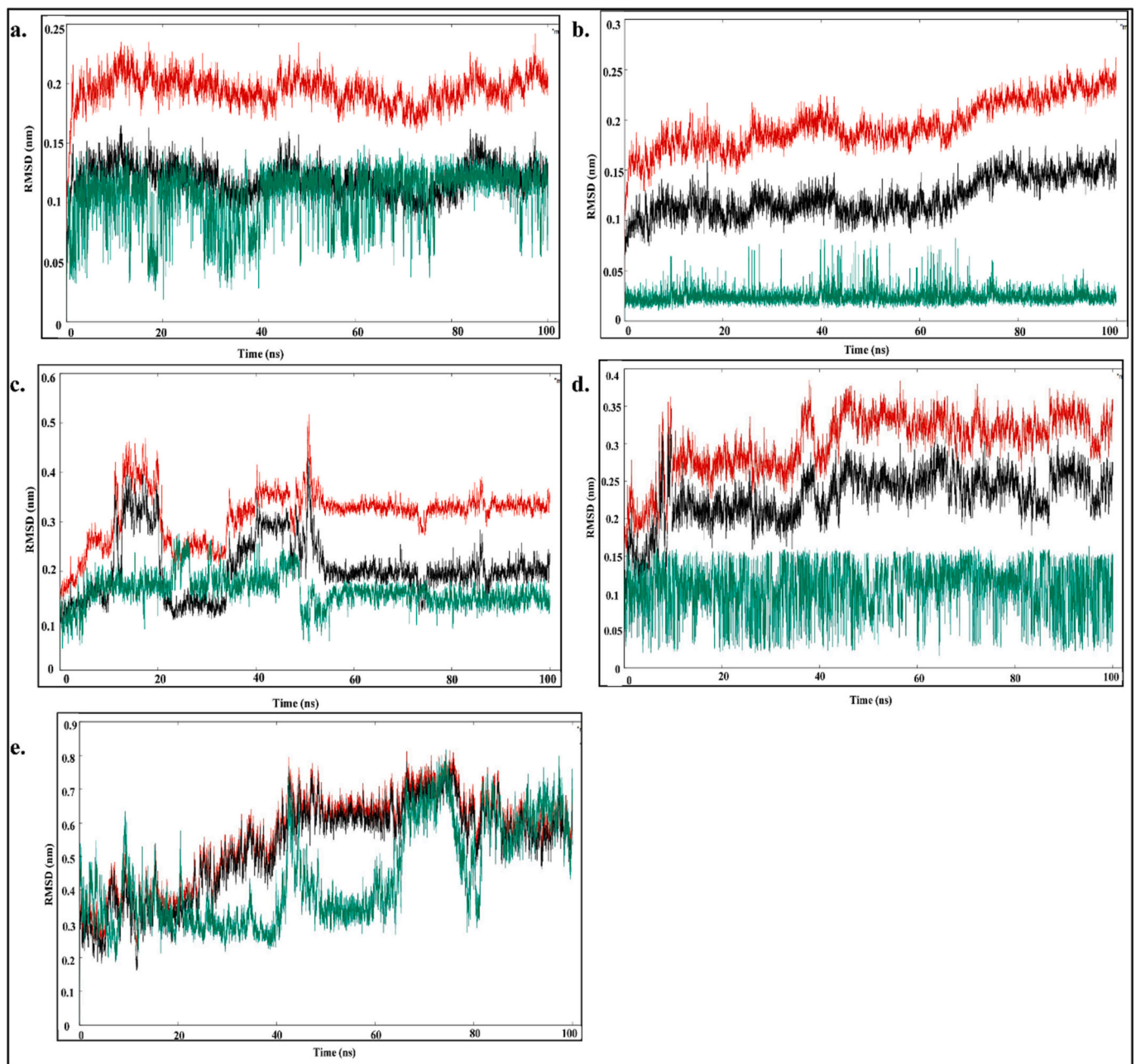


Fig. 2. Analysis of RMSD plots generated: (a) CHAPk- Glycyl-D-Alanine (b) CHAPk- Chitin, (c) SH3bk- Pentaglycine, (d) D-Ribitol-5-phosphate, (e) CHAPk-SH3bk-PG fragment. Black – protein, Red – protein + ligand, Green – ligand.

of CHAPk and CHAPk-SH3bk after 24-h of incubation (Fig. 4c). Also, the higher bacteriolytic activity of CHAPk was observed in comparison to CHAPk-SH3bk on planktonic cells for a short duration of treatment. Whereas, almost similar lytic activity was observed for novel chimeric endolysin CHAPk-SH3bk and CHAPk after 24-h treatment.

3.6. Stability of CHAPk-SH3bk at different storage temperatures

The thermostability of the CHAPk-SH3bk was determined and the result showed that CHAPk-SH3bk was highly active after 30 min of incubation at 4 °C (Fig. 4d). The endolysin maintained its lytic activity over a range of 20 °C to 37 °C. The incubation of endolysin at 50 °C and 70 °C caused complete inactivation of CHAPk-SH3bk.

3.7. Effect of pH on CHAPk-SH3bk

The incubation of CHAPk-SH3bk at different pH values displayed that lytic activity is maintained at pH 6; while at acidic pH 4 and at alkaline pH above 8, the chimeric endolysin loses its activity (Fig. 4e). The optimal pH range analyzed was (pH 6–pH 7.5).

3.8. Biofilm reduction activity of CHAPk and CHAPk-SH3bk

The biofilm reduction assay was analyzed using visual appearance in crystal-violet staining followed by measuring absorbance at OD_{570nm}. The biofilm reduction activity of CHAPk-SH3bk was higher than CHAPk. The CHAPk-SH3bk showed biofilm reduction activity against all the five *S. aureus* isolates with ~33 % activity against *S. aureus* (ATCC® BAA-44™) (Fig. 5b). CHAPk domain alone was able to lyse only two of the

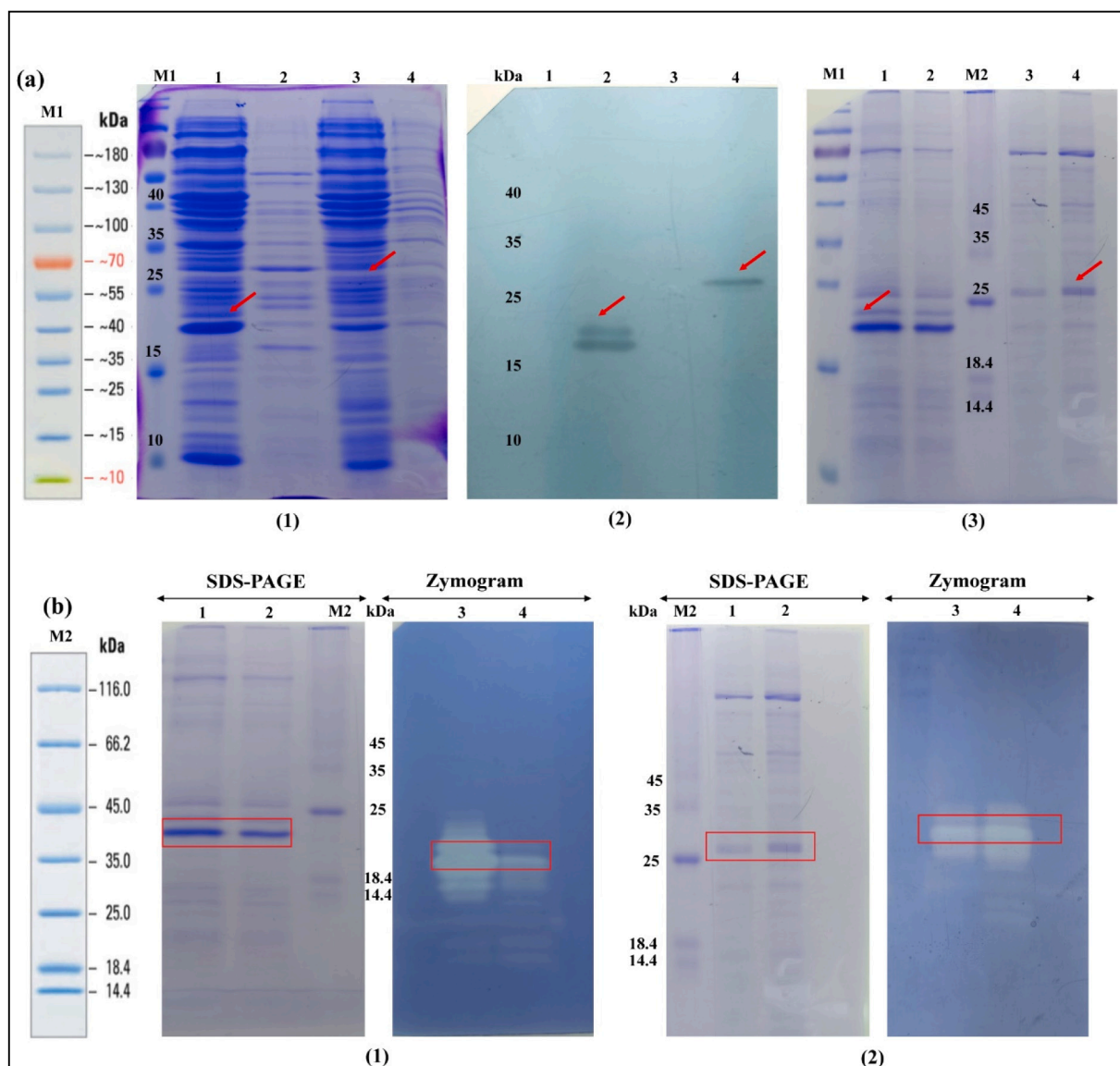


Fig. 3. SDS-PAGE, Western blot, and Zymogram analysis of CHAPk and CHAPk-SH3bk: (a) (1) SDS-PAGE: lane 1- induced CHAPk, lane 2- uninduced CHAPk, lane 3- induced CHAPk-SH3bk, and lane 4- uninduced CHAPk-SH3bk. (2) Western blot: lane 1- uninduced CHAPk, lane 2- induced CHAPk (band at 22.6 kDa), lane 3- uninduced CHAPk-SH3bk, and lane 4- induced CHAPk-SH3bk (band at 28 kDa). (3) SDS-PAGE: lane 1- purified CHAPk (10 μ g), lane 2- purified CHAPk (5 μ g), lane 3- purified CHAPk-SH3bk (5 μ g), and lane 4- purified CHAPk-SH3bk (10 μ g). (b) (1) Zymogram gel of CHAPk: lane 1- purified CHAPk (10 μ g), lane 2- purified CHAPk (5 μ g), lane 3- zone of clearance of 10 μ g CHAPk & lane 4 - zone of clearance of 5 μ g CHAPk. (2) Zymogram gel of CHAPk-SH3bk: lane 1- purified CHAPk-SH3bk (5 μ g), lane 2- purified CHAPk-SH3bk (10 μ g), lane 3- zone of clearance of 10 μ g CHAPk-SH3bk & lane 4 - zone of clearance of 5 μ g CHAPk-SH3bk. M1- PageRuler™ Prestained Protein Ladder (26616), M2- Pierce™ Unstained Protein MW Marker (26610).

five *S. aureus* isolates preformed biofilm. CHAPk showed no lytic activity against biofilm formed by hospital-associated *S. aureus* (ATCC® BAA-44™) (Fig. 5a). While 47 %, and 40 % of the reduction activity was displayed against biofilm formed by bovine origin *S. aureus* isolates SA1 and SA3 respectively. No significant activity of CHAPk was observed against preformed biofilms of isolates SA2, SA3, and SA4. The highest biofilm reduction activity of chimeric endolysin CHAPk-SH3bk of 60 % was displayed against bovine origin *S. aureus* isolate SA4. The biofilm reduction activity of 40 %, 20 %, and 30 % was observed against isolates SA1, SA2, and SA3, respectively. The crystal-violet staining results displayed clearing of biofilms after treatment with 0.05 μ g/ μ l CHAPk-SH3bk in all isolates as compared to biofilm growth in the negative control (Fig. 5c). Whereas, in the case of treatment with 0.05 μ g/ μ l CHAPk, biofilm reduction can be observed only in isolates SA1, and SA3. In conclusion, CHAPk-SH3bk was more effective against preformed biofilms of hospital-associated MRSA *S. aureus* (ATCC® BAA-44™) and

bovine origin MRSA isolates SA1, SA2, SA3, and SA4.

3.9. CLSM, COMSTAT, and SEM analysis

The DAPI-stained bacterial cells in the treated and untreated biofilms can be observed in Fig. 6. The interactive 3D surface plots of biofilms were prepared using ImageJ (Fig. S8). The COMSTAT results displayed the maximum thickness of untreated *S. aureus* (ATCC® BAA-44™), SA1, and SA4 biofilm was $9.19 \pm 0.69 \mu$ m, $17.25 \pm 1.84 \mu$ m, and $7.32 \pm 0.11 \mu$ m respectively. After treatment with CHAPk-SH3bk the maximum thickness of the ATCC® BAA-44™, and SA4 biofilm was found to be $4.46 \pm 0.50 \mu$ m, and $5.26 \pm 1.15 \mu$ m respectively. Whereas, after the subsequent treatment with CHAPk, the maximum thickness of biofilm formed by SA1, and ATCC® BAA-44™ was $3.19 \pm 0.34 \mu$ m and $7.59 \pm 1.03 \mu$ m respectively. The maximum thickness, biomass, and volume of microcolonies at the substratum of biofilms after treatment is mentioned

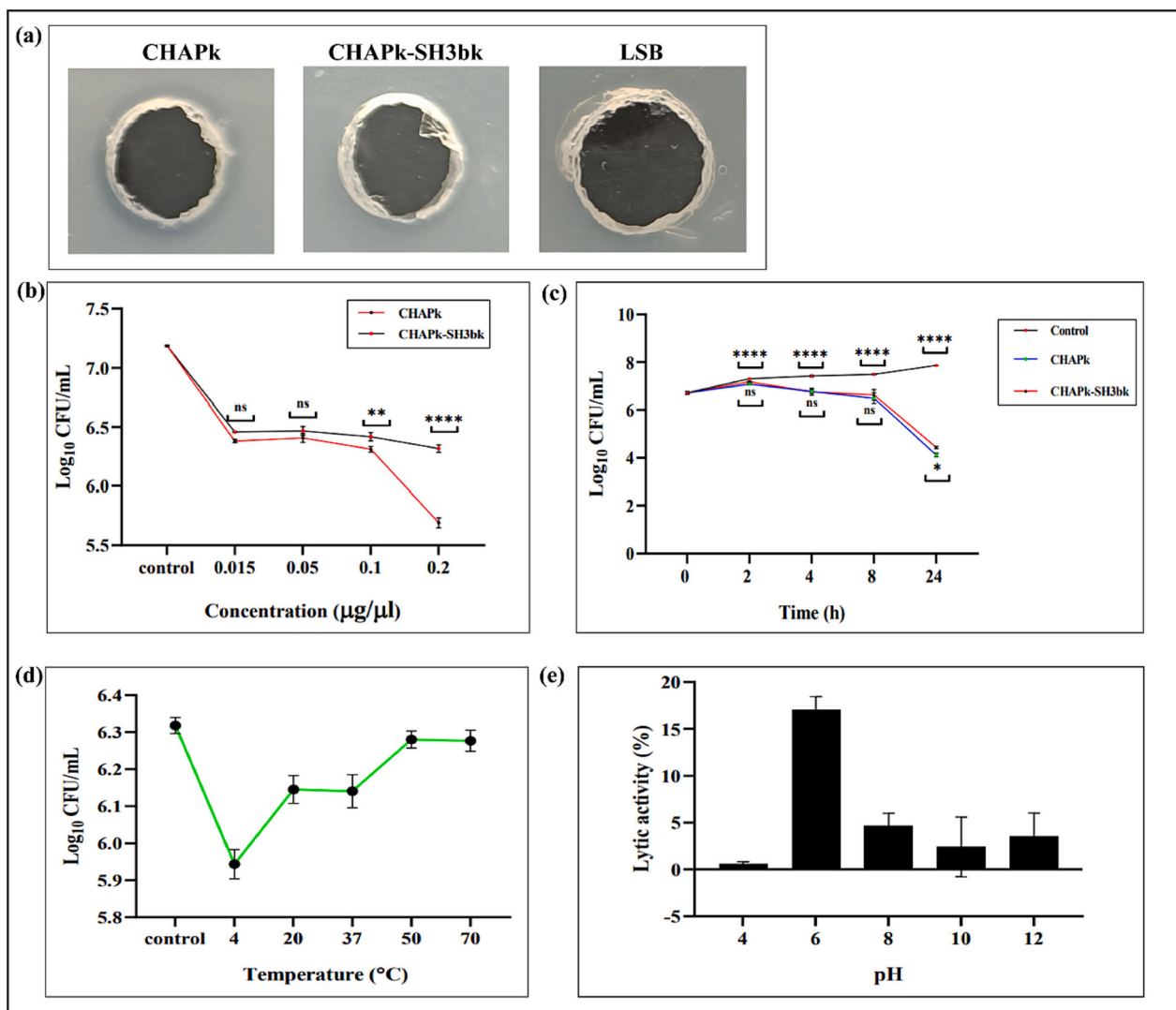


Fig. 4. Bactericidal activity of CHAPk and CHAPk-SH3bk against *Staphylococcus aureus* (ATCC® BAA-44™): (a) Diffusion of CHAPk (50 μg), CHAPk-SH3bk (50 μg), and LSB (50 μl) across agar containing heat-inactivated *S. aureus* (ATCC® BAA-44™). (b) Dose-dependent bacteriolytic efficacy of CHAPk and CHAPk-SH3bk against *S. aureus* (ATCC® BAA-44™) at different concentrations. (c) Time-dependent killing assay of CHAPk and CHAPk-SH3bk against *S. aureus* (ATCC® BAA-44™) at different time periods (0, 2, 4, 8, and 24 h). (d) Effect of temperature on the bacteriolytic stability of CHAPk-SH3bk against *S. aureus* (ATCC® BAA-44™). (e) Effect of pH on the bacteriolytic stability of CHAPk-SH3bk against *S. aureus* (ATCC® BAA-44™). The data are presented as the means \pm standard deviations of three replicates. Statistical significance was calculated using two-way ANOVA followed by Tukey's multiple comparison test. * $P < 0.05$; ** $P < 0.01$; **** $P < 0.0001$; ns, not significant.

in Tables 3a and 3b. The biofilm reduction ability of CHAPk-SH3bk was also analyzed using FESEM. As shown in Fig. 7(a-c), and (g-i), compact cell aggregation with thin biofilm matrix arranged in different layers was observed for the untreated *S. aureus* (ATCC® BAA-44™, and SA4) biofilms incubated for 24-h. Whereas, a significant decrease in the number and layers of the *S. aureus* cells was observed after treatment with 0.05 $\mu\text{g}/\mu\text{l}$ CHAPk-SH3bk Fig. 7(d, and j). Furthermore, after 18-h treatment a decrease and degradation of biofilm matrix was observed Fig. 7(e, f), and (k,l).

4. Discussion

S. aureus has developed antibiotic resistance against most of the commercially available antibiotics like oxacillin, vancomycin, etc. [32]. MRSA is emerging as a notorious pathogen because of its ability to form persistent biofilms on biotic and abiotic surfaces [33]. Previous studies have demonstrated that endolysins composed of EAD and CBD can disrupt preformed MRSA biofilms and act as promising biofilm

reduction agents [34,35]. The present study investigated the bacteriolytic and biofilm reduction ability of the gene encoding CHAPk (165 amino acids) domain of LysK endolysin from bacteriophage K and a novel chimeric LysK construct composed of CHAPk-SH3bk (250 amino acids). Bioinformatic analysis revealed that amino acid residues (ASP47, ASP56, and GLY74) within CHAP domain interact with Glycyl-D-Alanine, Chitin, and peptidoglycan-fragment, respectively were found to be highly conserved with a score of 9. The SH3b domain interacted with Pentaglycine forming hydrogen bonds with amino acids ASN15, GLU62, TYR83, and with D-Ribitol-5-phosphate at ARG87, indicating the conserved state of these amino acids with a score of 8–9 in ConSurf. The molecular docking studies were carried out to understand the interaction of CHAPk, and SH3bk domains with the bonds Glycyl-D-Alanine and pentaglycine respectively, as these bonds represent the activity site of these domains in the *S. aureus* peptidoglycan layer. The results were then compared to the insilico activity of novel chimeric endolysin CHAPk-SH3bk. The docking results displayed that the interaction of critical amino acids ASP47, ASP56, ARG71, and GLY74 of the

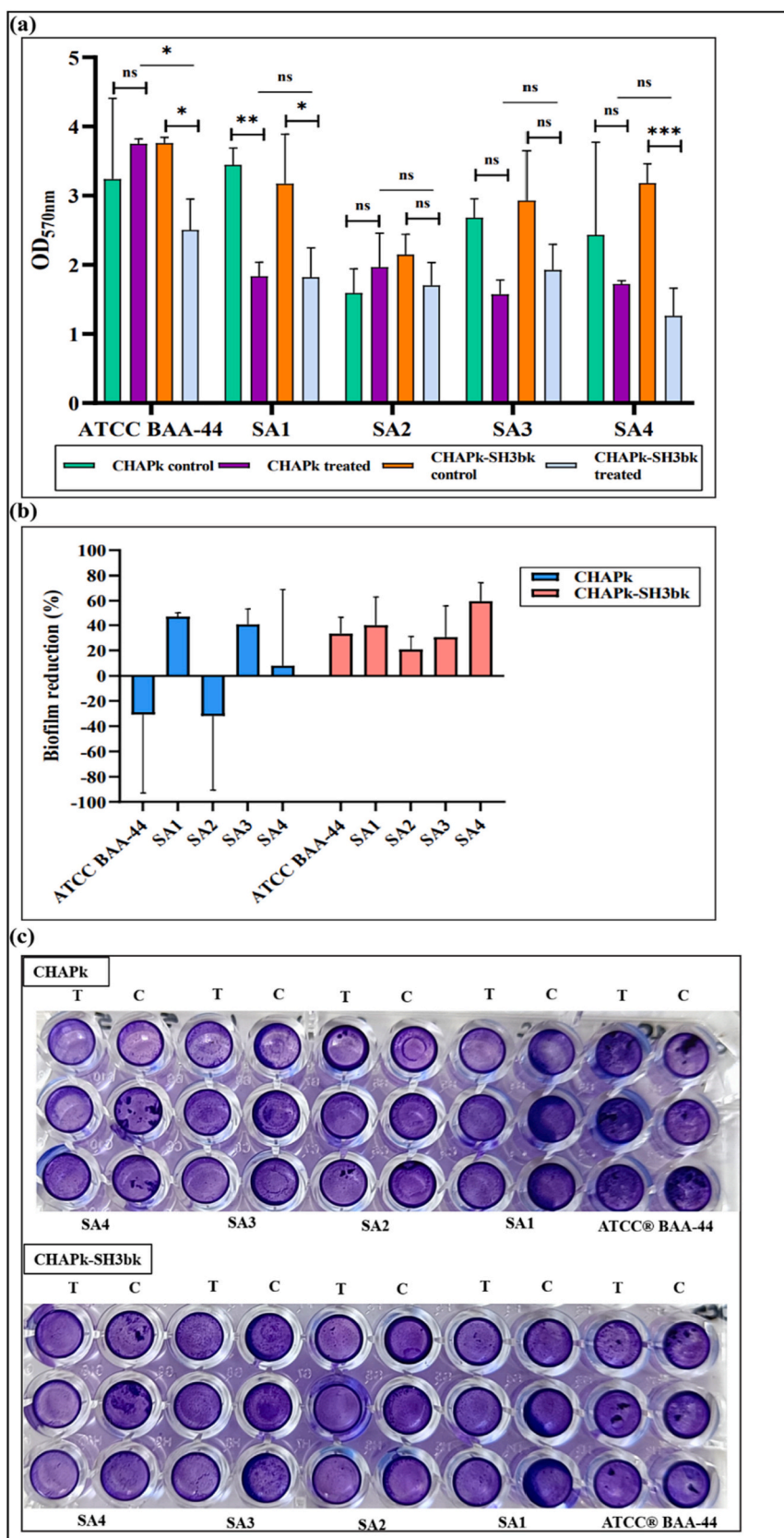


Fig. 5. Biofilm reduction activity of CHAPk and CHAPk-SH3bk. **(a)** The graph represents OD_{570nm} value for bacterial cells adhered to wells after treatment of biofilm for 18-h at 37 °C. **(b)** Graph representing the percentage of biofilm reduced using 0.05 µg/µl of CHAPk and CHAPk-SH3bk as treatment for 24-h biofilm. **(c)** Crystal violet staining of treated biofilms. C- negative control, T- treated. The data are presented as the means±standard deviations of three replicates. Statistical significance was calculated using two-way ANOVA followed by Tukey's multiple comparison test. *P < 0.05; **P < 0.01; ****P < 0.0001; ns, not significant.

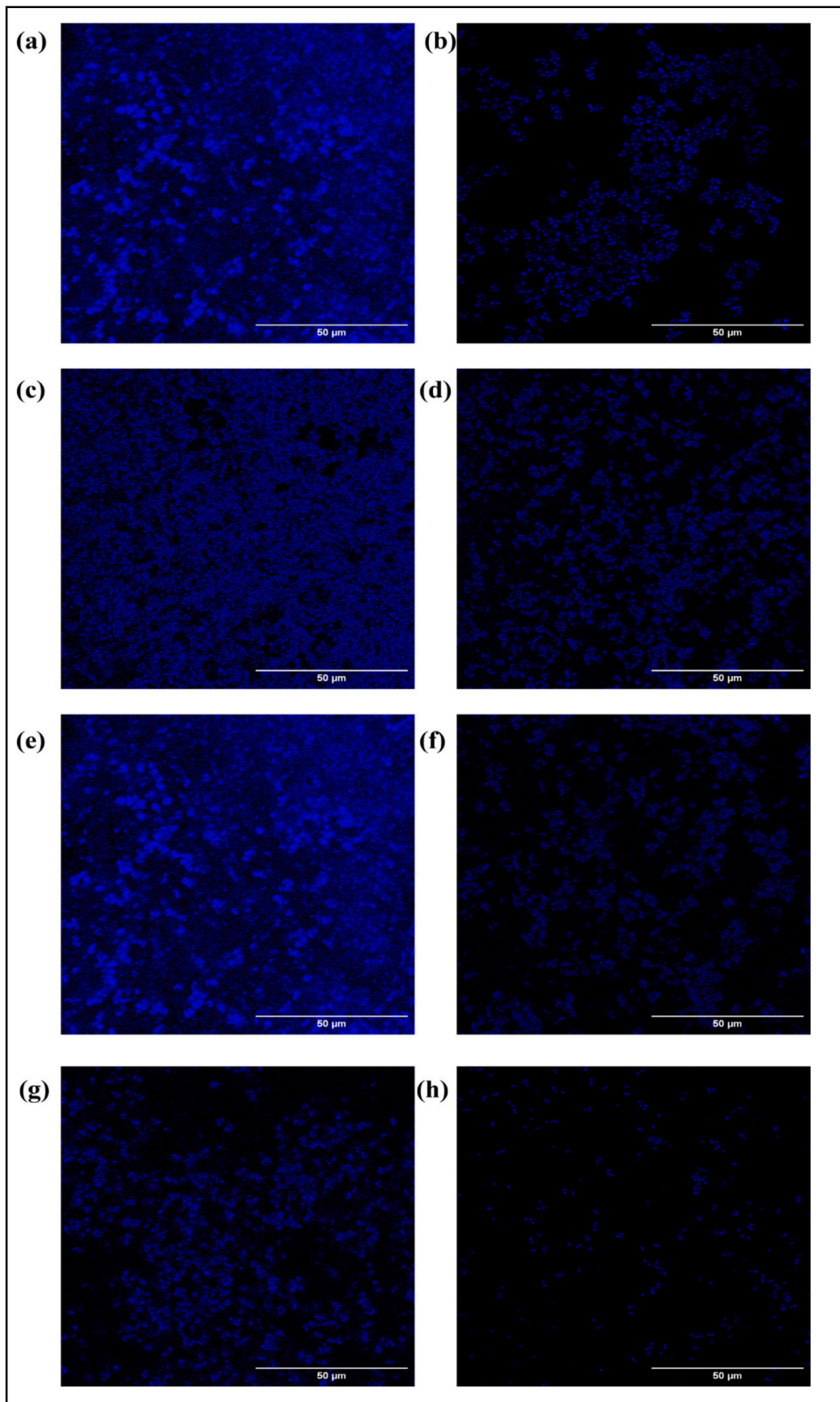


Fig. 6. CLSM analyses of the lytic activity of CHAPk, and CHAPk-SH3bk on 24-h preformed biofilms. (a) 24 h biofilm control (ATCC® BAA-44™), (b) ATCC® BAA-44™ biofilm treated with 0.05 $\mu\text{g}/\mu\text{l}$ CHAPk-SH3bk, (c) 24 h biofilm control (SA4), (d) SA4 biofilm treated with 0.05 $\mu\text{g}/\mu\text{l}$ CHAPk-SH3bk, (e) 24 h biofilm control (ATCC® BAA-44™), (f) ATCC® BAA-44™ biofilm treated with 0.05 $\mu\text{g}/\mu\text{l}$ CHAPk, (g) 24 h biofilm control (SA1), (h) SA1 biofilm treated with 0.05 $\mu\text{g}/\mu\text{l}$ CHAPk.

Table 3a

Maximum thickness, biomass, and Volume of microcolonies at the substratum of biofilms after treatment with CHAPk-SH3bk analyzed using COMSTAT.

S. No	Sample Name	CHAPk-SH3bk					
		Control			Treated		
		Maximum thickness (μm)	Biomass ($\mu\text{m}^3/\mu\text{m}^2$)	Average volume of colonies at substratum (μm^3)	Maximum thickness (μm)	Biomass ($\mu\text{m}^3/\mu\text{m}^2$)	Average volume of colonies at substratum (μm^3)
1.	ATCC®BAA-44™	9.19 ± 0.69	3.43017	22,294.32	4.46 ± 0.50	2.05252	5141.6118
2.	SA4	7.32 ± 0.11	3.15735	38,239.55	5.26 ± 1.15	1.82908	21,037.93

Table 3b

Maximum thickness, biomass, and Volume of microcolonies at the substratum of biofilms after treatment with CHAPk analyzed using COMSTAT.

S. No	Sample Name	CHAPk					
		Control			Treated		
		Maximum thickness (μm)	Biomass ($\mu\text{m}^3/\mu\text{m}^2$)	Average volume of colonies at substratum (μm^3)	Maximum thickness (μm)	Biomass ($\mu\text{m}^3/\mu\text{m}^2$)	Average volume of colonies at substratum (μm^3)
1.	ATCC®BAA-44™	9.19 ± 0.69	3.43017	22,294.32	7.59 ± 1.03	2.53554	13,973.8535
2.	SA1	17.25 ± 1.84	7.24364	34,449.0273	3.19 ± 0.34	1.02547	4288.4839

CHAPk domain is maintained in the chimeric endolysin CHAPk-SH3bk. Additionally, the molecular docking studies showed the interaction of the SH3bk domain with *S. aureus* cell wall teichoic acid component (D-Ribitol-5-phosphate) using four amino acids. The MD simulation results for the same represented a maximum of 5 hydrogen bonds between D-Ribitol-5-phosphate and SH3b domain with 3 hydrogen bonds remaining during most of the 100 ns run time. Also, in comparison to pentaglycine; SH3bk showed a more stable interaction with D-Ribitol-5-phosphate as can be observed from RMSF, RMSD, and Rg plots of both the complexes. This interaction of the SH3b domain with the WTA component can be explored for diagnosis of Gram-positive bacteria and therapeutic studies as earlier explored in the case of *Listeria* spp. [36]. The CHAP domain alone formed a maximum of 6 hydrogen bonds with Glycyl-D-Alanine and Chitin, whereas chimeric construct CHAPk-SH3bk displayed interaction with peptidoglycan fragment using a maximum of 14 hydrogen bonds with a minimum of 8 hydrogen bonds during the run time of 100 ns. This signifies a better interaction of the CHAPk-SH3bk domain with the peptidoglycan layer of Gram-positive bacteria, which may lead to better bacteriolytic activity of the chimeric construct than the CHAPk domain alone. The solubility of a protein is important for its stability and therapeutic usage [37]. In this study, the pET-22b(+) vector was used to ensure that expressed CHAPk and CHAPk-SH3bk were properly folded, purified, and soluble. The presence of N-terminal pelB signal sequence facilitated the expression of proteins in the periplasmic localization instead of inclusion body formation, which can be easily purified with the help of C-terminal 6 × His-tag [38]. The zymogram and diffusion lysis assay showed bacteriolytic activity of expressed CHAPk and CHAPk-SH3bk by the development of clear zones on heat-killed *S. aureus*. Also, the purified CHAPk and CHAPk-SH3bk displayed lytic activity against clinical isolates of MRSA. The decrease in the CFU/ml of MRSA bacteria with increased concentration of endolysin CHAPk shows the effectiveness of this single-domain endolysin against planktonic bacterial culture. The results of the bactericidal activity assay results displayed no significant difference between the activity of CHAPk and CHAPk-SH3bk when used in concentrations 0.015 $\mu\text{g}/\mu\text{l}$, and 0.05 $\mu\text{g}/\mu\text{l}$. However, a significant difference was observed when 0.1 $\mu\text{g}/\mu\text{l}$ ($p \leq 0.05$), and 0.2 $\mu\text{g}/\mu\text{l}$ ($p \leq 0.0001$) of lytic proteins were used for 2-h incubation period. Bactericidal assay results displayed higher activity of CHAPk as compared to chimeric endolysin CHAPk-SH3bk with 2- \log_{10} reduction in cell forming units in 2-h of incubation. Earlier studies have reported the lytic activity of CHAPk

domain in combination with cell wall binding domain like endolysin PRF-119, and HY-133 composed of LysK CHAP domain and cell wall binding domain of Lysostaphin [39,40]. It was found that both combinations were effective against MRSA. While there are no previous studies of CHAPk in combination with the LysK SH3b domain, this study showed that the treatment of CHAPk-SH3bk for 24 h significantly reduced MRSA by $\sim 3.5\text{-log}_{10}$ units ($p < 0.05$). Although, no significant difference in the activity of CHAPk-SH3bk and CHAPk was observed in the time-kill experiment for the first 8 h. Time kill kinetics results showed that the lytic activity of CHAPk is retained in the presence of SH3b domain in the construct CHAPk-SH3bk. Becker et al. [17] demonstrated that the CHAP domain conjugated to LysK221 and small fragment of Amidase (amino acid 197–221) did not result in better lytic activity but significantly increased in activity when CHAP is conjugated to both amidase domain (amino acid 197–221) as well as SH3b domain. This implies that the presence of the cell wall binding domain does not necessarily inhibit the lytic activity of the enzymatically active domain but rather enhances its activity. The temperature and pH play an important role in the stability and activity of the protein for therapeutic usage or biopreservation [41]. This study reports that CHAPk-SH3bk is highly active at 4 °C and maintains its activity in the range of 20–37 °C, which represents the optimal human body temperature. While CHAPk-SH3bk is nearly inactive at temperatures above 50 °C, which is similar to the activity of the CHAPk as determined by Fenton et al. [42]; with no activity of CHAPk above 45 °C. The dependency of biological processes on pH makes it necessary to determine the optimal pH for the activity of expressed novel endolysin CHAPk-SH3bk. In this study, we found that CHAPk-SH3bk was active in the range pH 6–7.5 which is the normal range for human body fluids. It was observed that at high acidic (pH 4) and in alkaline pH (pH 8); the activity of CHAPk-SH3bk was decreased. Conversely, Fenton et al. found CHAPk to be most active at pH 9 (Table S2) [42].

To analyze if the combination of SH3bk domain with CHAPk exhibits enhanced lytic activity against sessile MRSA forming biofilm, four MRSA isolated from bovine mastitis cases and one MRSA ATCC® BAA-44™ (isolated from hospital in Lisbon, Portugal) were selected. The results displayed high biofilm reduction activity of CHAPk-SH3bk against MRSA ATCC® BAA-44™. The CHAPk-SH3bk reduced $\sim 33\%$ of the biofilm formed with a concentration of 0.05 $\mu\text{g}/\mu\text{l}$ over 24 h of incubation, while there was no visible reduction on the preformed biofilm due to the activity of CHAPk. The results displayed no significant

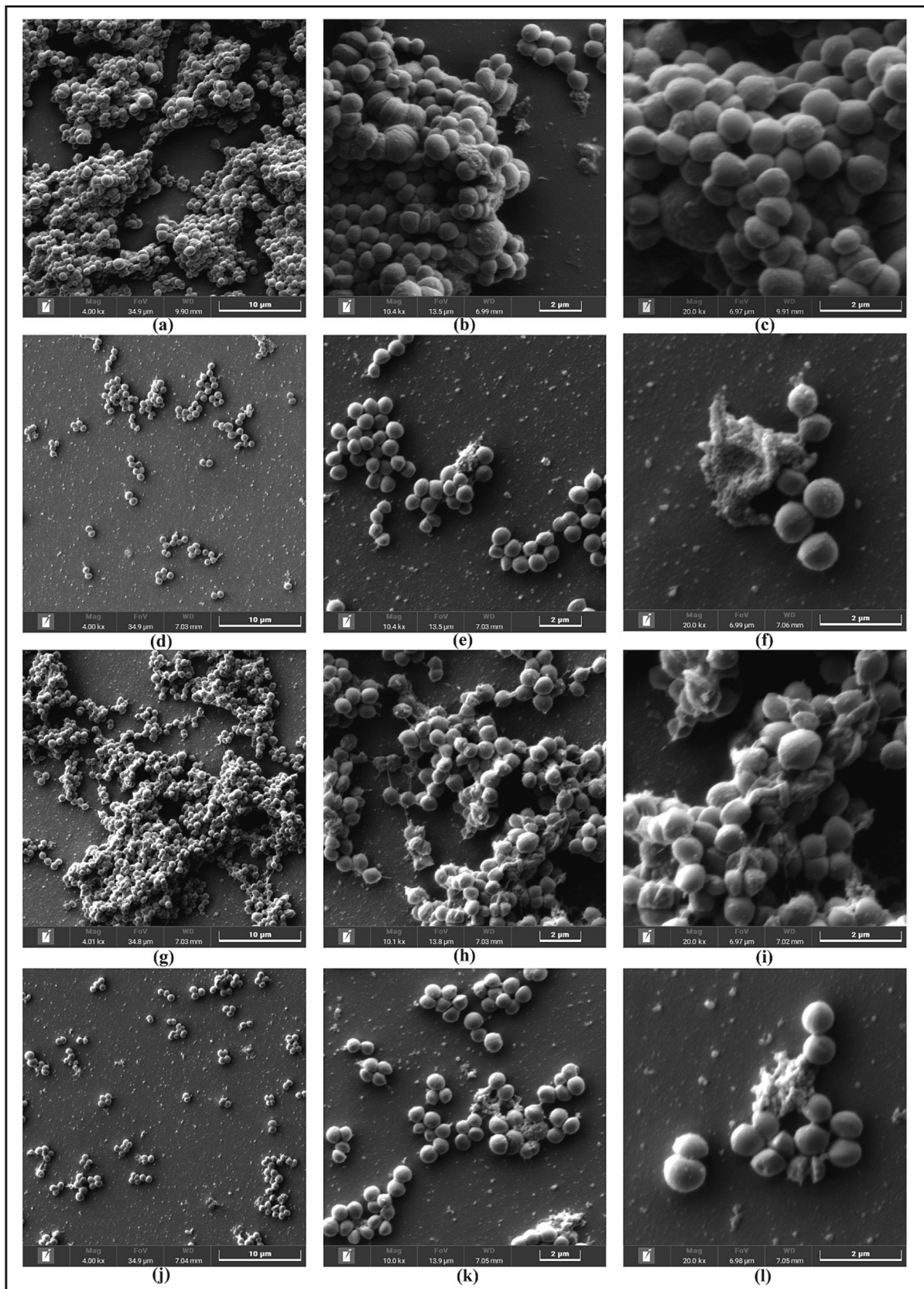


Fig. 7. SEM analyses of the lytic action of CHAPk, and CHAPk-SH3bk. (a–c) 24 h biofilm control (ATCC® BAA-44™), (d–f) ATCC® BAA-44™ biofilm treated with 0.05 µg/µl CHAPk-SH3bk, (g–i) 24 h biofilm control (SA4), (j–l) SA4 biofilm treated with 0.05 µg/µl CHAPk-SH3bk.

difference between CHAPk negative control and CHAPk-treated biofilm formed by ATCC® BAA-44™. There are no previous studies of the antibiofilm activity of CHAPk on MRSA from human or hospital origin. Olsen et al. [43] studied the effect of full endolysin LysK on biofilm formed by *S. aureus* [SA113 (ATCC 35556)] isolated from conjunctiva, corneal ulcer and found that LysK reduced >40 % of the biofilm formed. Biofilm reduction activity of CHAPk against *S. aureus* of bovine origin (*S. aureus* strain DPC5246) has been studied by Fenton et al. [44], and they found that CHAPk (31.25 µg/ml) can remove *Staphylococcal* biofilm completely with an incubation time of 4 h. In contradiction, the MRSA isolates of bovine origin used in our study (SA2, SA3, and SA4) displayed no significant difference in bacterial cell concentration before and after CHAPk treatment and only a significant biofilm reduction of 47 % ($P \leq 0.01$) was observed against SA1 after CHAPk treatment. Whereas, in comparison to CHAPk, CHAPk-SH3bk displayed a significant difference in biofilm formation against two MRSA isolates SA1, and SA4. The present study revealed the potential of novel chimeric endolysin CHAPk-SH3bk against biofilm formed by MRSA bacteria of both hospital and bovine origin with biofilm reduction ability ranging from 20 %–60 %. Also, CHAPk-SH3bk is more efficient in the removal of biofilms as compared to CHAPk. This study recommends the use of CHAPk-SH3bk for the lysis of biofilm-forming MRSA and destruction of preformed MRSA biofilms on hospital related medical equipment, glassware's. This study also provides evidence that CHAPk-SH3bk should be studied and explored more for the treatment of bovine mastitis associated-MRSA resistant to antibiotics that is difficult to treat because of the biofilm formation in the udder.

5. Conclusion

The present study demonstrated bioinformatic analysis, cloning, expression, purification, and bacteriolytic activity of novel chimeric endolysin CHAPk-SH3bk against planktonic and sessile MRSA. It was found that CHAPk-SH3bk was more effective than CHAPk against preformed biofilms of MRSA from hospital and bovine origin in in-vitro conditions. Bactericidal and time-kill assay displayed that the presence of cell wall binding domain SH3bk enhanced the activity of enzymatically active domain CHAPk against sessile MRSA. Overall, this study provides a reference for using CHAPk-SH3bk chimeric endolysin as an alternative to antibiotics to combat MRSA-associated biofilms persistent in hospital devices. Further studies are needed to exploit the full potential of this chimeric endolysin in combination with other antimicrobial agents and explore its efficacy in in-vivo conditions for therapeutic usage in MRSA-associated infections in animals and humans.

CRedit authorship contribution statement

Manisha Behera: Conceptualization, Data curation, Formal analysis, Investigation, Writing – original draft. **Gagandeep Singh:** Software, Writing – review & editing. **Ashutosh Vats:** Methodology, Visualization. **Parmanand:** Data curation, Investigation. **Mayank Roshan:** Resources. **Devika Gautam:** Visualization. **Chanchal Rana:** Resources. **Rajesh Kumar Kesharwani:** Software, Writing – review & editing. **Sachinandan De:** Supervision, Writing – review & editing. **Soma M. Ghorai:** Project administration, Supervision, Writing – review & editing.

Declaration of competing interest

Authors declare no competing interest.

Data availability

Data will be made available on request.

Acknowledgments

We thank Principal, Hindu College, University of Delhi, for providing infrastructural facilities. We acknowledge Council of Scientific and Industrial Research, India (CSIR) for financial support in the form of research fellowship to Manisha Behera (08/555(0001)/2019-EMR-I). The authors also thank Dr. Sachinandan De (National Dairy Research Institute, Karnal) for support and guidance. Authors also thank Confocal laser scanning microscopy, and field emission scanning electron microscopy facility at Central Instrumentation Facility (CIF), University of Delhi South Campus, Delhi, India for their help and support.

Appendix A. Supplementary data

Supplementary data to this article can be found online at <https://doi.org/10.1016/j.ijbiomac.2023.127969>.

References

- [1] B.P. Howden, S.G. Giulieri, T. Wong Fok Lung, S.L. Baines, L.K. Sharkey, J.Y.H. Lee, A. Hachani, I.R. Monk, T.P. Stinear, *Staphylococcus aureus* host interactions and adaptation, *Nat. Rev. Microbiol.* 21 (2023), <https://doi.org/10.1038/s41579-023-00852-y>.
- [2] C. Laux, A. Peschel, B. Krismer, *Staphylococcus aureus* colonization of the human nose and interaction with other microbiome members, *Microbiol. Spectr.* 7 (2019), <https://doi.org/10.1128/MICROBIOLSPPEC.GPP3-0029-2018/ASSET/A48D6709-0E73-40D0-B16A-AD40534CF67A/ASSETS/GRAPHIC/GPP3-0029-2018-FIG 2.GIF>.
- [3] N.A. Turner, B.K. Sharma-kuinkel, S.A. Maskarinec, E.M. Eichenberger, P.P. Shah, M. Carugati, T.L. Holland, V.G. Fowler, Methicillin-resistant *Staphylococcus aureus*: an overview of basic and clinical research, *Nat. Rev. Microbiol.* 17 (2019) 203–218, <https://doi.org/10.1038/s41579-018-0147-4>.
- [4] A.S. Lee, H. De Lencastre, J. Garau, J. Kluytmans, S. Malhotra-kumar, A. Peschel, S. Harbarth, Methicillin-resistant *Staphylococcus aureus*, *Nat. Publ. Group* 4 (2018) 1–23, <https://doi.org/10.1038/nrdp.2018.33>.
- [5] J. Bhavana, N.K. Rama, Study of HA-MRSA and CA-MRSA isolated from clinical cases in a tertiary care hospital, *Indian J. Public Heal. Res. Dev.* 8 (2017) 106–111, <https://doi.org/10.5958/0976-5506.2017.00092.4>.
- [6] D.E. Moormeier, K.W. Bayles, *Staphylococcus aureus* biofilm: a complex developmental organism, (n.d.). doi:<https://doi.org/10.1111/mmi.13634>.
- [7] R. Parastan, M. Kargar, K. Solhjo, F. Kafizadeh, *Staphylococcus aureus* Biofilms: Structures, Antibiotic Resistance, Inhibition, and Vaccines, 2020, <https://doi.org/10.1016/j.genrep.2020.100739>.
- [8] M. Frieri, K. Kumar, A. Boutin, Antibiotic resistance, *J. Infect. Public Health* 10 (2017) 369–378, <https://doi.org/10.1016/j.jiph.2016.08.007>.
- [9] R.R. Pedersen, V. Krömker, T. Bjarnsholt, K. Dahl-Pedersen, R. Buhl, E. Jørgensen, Biofilm research in bovine mastitis, *Front. Vet. Sci.* 8 (2021), 656810, <https://doi.org/10.3389/FVETS.2021.656810/BIBTEX>.
- [10] K.M. Craft, J.M. Nguyen, L.J. Berg, S.D. Townsend, Methicillin-resistant *Staphylococcus aureus* Phenotype, 2019, <https://doi.org/10.1039/c9md00044e>.
- [11] F.L.G. Altamirano, crossm Phage Therapy in the Postantibiotic Era, Downloaded from, <http://cmr.asm.org/>. on February 21, 2021 at 32, National Dairy Research Institute, , pp. 1–25.
- [12] H. Haddad Kashani, M. Schmelcher, H. Sabzalipoor, E. Seyed Hosseini, R. Moniri, Recombinant endolysins as potential therapeutics against antibiotic-resistant *Staphylococcus aureus*: current status of research and novel delivery strategies, *Clin. Microbiol. Rev.* 31 (2018), <https://doi.org/10.1128/CMR.00071-17>.
- [13] D. Gutiérrez, L. Fernández, A. Rodríguez, P. García, Are phage lytic proteins the secret weapon to kill *Staphylococcus aureus*? *MBio* 9 (2018) 1–17, <https://doi.org/10.1128/mBio.01923-17>.
- [14] M. Schmelcher, Y. Shen, D.C. Nelson, M.R. Eugster, F. Eichenseher, D.C. Hanke, M. J. Loessner, S. Dong, D.G. Pritchard, J.C. Lee, S.C. Becker, J. Foster-Frey, D. M. Donovan, Evolutionarily distinct bacteriophage endolysins featuring conserved peptidoglycan cleavage sites protect mice from MRSA infection, *J. Antimicrob. Chemother.* 70 (2014) 1453–1465, <https://doi.org/10.1093/jac/dku552>.
- [15] M. Horgan, G. O'Flynn, J. Garry, J. Cooney, A. Coffey, G.F. Fitzgerald, R. Paul Ross, O. McAuliffe, Phage lysin LysK can be truncated to its CHAP domain and retain lytic activity against live antibiotic-resistant *Staphylococci*, *Appl. Environ. Microbiol.* 75 (2009) 872–874, <https://doi.org/10.1128/AEM.01831-08>.
- [16] H.H. Kashani, H. Fahimi, Y.D. Goli, R. Moniri, A novel chimeric endolysin with antibacterial activity against methicillin-resistant *Staphylococcus aureus*, *Front. Cell. Infect. Microbiol.* 7 (2017) 1–12, <https://doi.org/10.3389/fcimb.2017.00290>.
- [17] S.C. Becker, S. Dong, J.R. Baker, J. Foster-frey, D.G. Pritchard, D.M. Donovan, LysK CHAP Endopeptidase Domain Is Required for Lysis of Live *Staphylococcal* Cells 294, 2009, pp. 52–60, <https://doi.org/10.1111/j.1574-6968.2009.01541.x>.
- [18] M. Schmelcher, A.M. Powell, S.C. Becker, M.J. Camp, D.M. Donovan, Chimeric phage lysins act synergistically with lysostaphin to kill mastitis-causing *Staphylococcus aureus* in murine mammary glands, *Appl. Environ. Microbiol.* 78 (2012) 2297–2305, https://doi.org/10.1128/AEM.07050-11/SUPPL_FILE/AEM-AEM07050-11-S01.PDF.

- [19] J. Mao, M. Schmelcher, W.J. Harty, J. Foster-Frey, D.M. Donovan, Chimeric Ply187 endolysin kills *Staphylococcus aureus* more effectively than the parental enzyme, *FEMS Microbiol. Lett.* 342 (2013) 30–36, <https://doi.org/10.1111/1574-6968.12104>.
- [20] M. Roshan, D. Arora, M. Behera, A. Vats, D. Gautam, R. Deb, T. Parkunan, S. De, Comparative immunology, microbiology and infectious diseases virulence and enterotoxin gene profile of methicillin-resistant *Staphylococcus aureus* isolates from bovine mastitis, *Comp. Immunol. Microbiol. Infect. Dis.* 80 (2022), 101724, <https://doi.org/10.1016/j.cimid.2021.101724>.
- [21] P. Mitkowski, E. Jagielska, E. Nowak, J.M. Bujnicki, F. Stefaniak, D. Niedziatek, M. Bochtler, I. Sabała, Structural bases of peptidoglycan recognition by lysostaphin SH3b domain, *Sci. Rep.* 9 (2019) 1–14, <https://doi.org/10.1038/s41598-019-42435-z>.
- [22] M.J. Abraham, T. Murtola, R. Schulz, S. Páll, J.C. Smith, B. Hess, E. Lindahl, ScienceDirect GROMACS: High Performance Molecular Simulations Through Multi-level Parallelism From Laptops to Supercomputers, 2015, <https://doi.org/10.1016/j.softx.2015.06.001>.
- [23] G. Singh, H. Soni, S. Tandon, V. Kumar, G. Babu, V. Gupta, P. (Chattopadhyay) Chaudhuri, Identification of natural DHFR inhibitors in MRSA strains: structure-based drug design study, *Results Chem.* 4 (2022), 100292, <https://doi.org/10.1016/J.RECHEM.2022.100292>.
- [24] M. Piuri, G.F. Hatfull, A peptidoglycan hydrolase motif within the mycobacteriophage TM4 tape measure protein promotes efficient infection of stationary phase cells, *Mol. Microbiol.* 62 (2006) 1569–1585, <https://doi.org/10.1111/J.1365-2958.2006.05473.X>.
- [25] F. Oechslin, C. Menzi, P. Moreillon, G. Resch, The multidomain architecture of a bacteriophage endolysin enables intramolecular synergism and regulation of bacterial lysis, *J. Biol. Chem.* 296 (2021), 100639, <https://doi.org/10.1016/j.jbc.2021.100639>.
- [26] L. Rodríguez, B. Martínez, Y. Zhou, A. Rodríguez, D.M. Donovan, P. García, Lytic activity of the virion-associated peptidoglycan hydrolase HydH5 of *Staphylococcus aureus* bacteriophage vB-SauS-phiPLA88, *BMC Microbiol.* 11 (2011) 1–11, <https://doi.org/10.1186/1471-2180-11-138/FIGURES/6>.
- [27] N. Lu, Y. Sun, Q. Wang, Y. Qiu, Z. Chen, Y. Wen, S. Wang, Y. Song, Cloning and characterization of endolysin and holin from *Streptomyces avermitilis* bacteriophage phiSASD1 as potential novel antibiotic candidates, *Int. J. Biol. Macromol.* 147 (2020) 980–989, <https://doi.org/10.1016/j.ijbiomac.2019.10.065>.
- [28] J.A. Wu, C. Kusuma, J.J. Mond, J.F. Kokai-Kun, Lysostaphin disrupts *Staphylococcus aureus* and *Staphylococcus epidermidis* biofilms on artificial surfaces, *Antimicrob. Agents Chemother.* 47 (2003) 3407–3414, <https://doi.org/10.1128/AAC.47.11.3407-3414.2003>.
- [29] M. Daniela, H. Oliveira, A. Faustino, S. Sillankorva, Characterization of MSlys, the endolysin of *Streptococcus pneumoniae* phage MS1, *Biotechnol. Rep.* 28 (2020).
- [30] M.D. Abràmoff, I. Hospitals, P.J. Magalhães, M. Abràmoff, *Image Processing With ImageJ*, *Biophotonics Int.* 2004.
- [31] A. Heydorn, A.T. Nielsen, M. Hentzer, M. Givskov, B.K. Ersbøll, S. Molin, Quantification of biofilm structures by the novel computer program COMSTAT, *Microbiology* 2395–2407 (2000).
- [32] M. Vestergaard, D. Frees, H. Ingmer, Antibiotic resistance and the MRSA problem, *Microbiol. Spectr.* 7 (2019), <https://doi.org/10.1128/MICROBIOLSP.0057-2018>.
- [33] S. Cascioferro, D. Carbone, B. Parrino, C. Pecoraro, E. Giovannetti, G. Cirrincione, P. Diana, Therapeutic strategies to counteract antibiotic resistance in MRSA biofilm-associated infections, *ChemMedChem* 16 (2021) 65–80, <https://doi.org/10.1002/CMDC.202000677>.
- [34] S.B. Linden, H. Zhang, R.D. Heselpoth, Y. Shen, M. Schmelcher, F. Eichenseher, D. C. Nelson, Biochemical and biophysical characterization of PlyGRCS, a bacteriophage endolysin active against methicillin-resistant *Staphylococcus aureus*, *Appl. Microbiol. Biotechnol.* 99 (2015) 741–752, <https://doi.org/10.1007/s00253-014-5930-1>.
- [35] Y. Lu, Y. Wang, J. Wang, Y. Zhao, Q. Zhong, G. Li, Z. Fu, S. Lu, Phage endolysin LysP108 showed promising antibacterial potential against methicillin-resistant *Staphylococcus aureus*, *Front. Cell. Infect. Microbiol.* 11 (2021) 1–12, <https://doi.org/10.3389/fcimb.2021.668430>.
- [36] Y. Shen, I. Kalograiaki, A. Prunotto, M. Dunne, S. Boulos, N.M.I. Taylor, E. Sumrall, M.R. Eugster, R. Martin, A. Julian-Rodero, B. Gerber, P.G. Leiman, M. Menéndez, M.D. Peraro, F.J. Cañada, M.J. Loessner, Molecular Basis for Recognition of *Listeria* Cell Wall Teichoic Acid by the Pseudo-symmetric SH3b-like Repeats of a Bacteriophage Endolysin, *bioRxiv*, 2020, 2020.06.05.136911, <http://biornxiv.org/content/early/2020/06/05/2020.06.05.136911.abstract>.
- [37] L. Grossmann, D.J. McClements, Current insights into protein solubility: a review of its importance for alternative proteins, *Food Hydrocoll.* 137 (2023), 108416, <https://doi.org/10.1016/J.FOODHYD.2022.108416>.
- [38] Novagen, pET System Manual, 11th edition, 2005. www.novagen.com (toegang verkry 03 Julie 2023).
- [39] E.A. Idelevich, C. Von Eiff, A.W. Friedrich, D. Iannelli, G. Xia, G. Peters, A. Peschel, I. Wanninger, K. Becker, In vitro activity against *Staphylococcus aureus* of a novel antimicrobial agent, PRF-119, a recombinant chimeric bacteriophage endolysin, *Antimicrob. Agents Chemother.* 55 (2011) 4416–4419, <https://doi.org/10.1128/AAC.00217-11>.
- [40] E.A. Idelevich, F. Schaumburg, D. Knaack, A.S. Scherzinger, W. Mutter, G. Peters, A. Peschel, K. Becker, The recombinant bacteriophage endolysin HY-133 exhibits in vitro activity against different African clonal lineages of the *Staphylococcus aureus* complex, including *Staphylococcus schweitzeri*, *Antimicrob. Agents Chemother.* 60 (2016) 2551–2553, <https://doi.org/10.1128/AAC.02859-15>.
- [41] K. Talley, E. Alexov, On the pH-optimum of activity and stability of proteins, *Proteins* 78 (2010) 2699–2706, <https://doi.org/10.1002/PROT.22786>.
- [42] M. Fenton, R.P. Ross, O. McAuliffe, J. O'Mahony, A. Coffey, Characterization of the staphylococcal bacteriophage lysin CHAP(K), *J. Appl. Microbiol.* 111 (2011) 1025–1035, <https://doi.org/10.1111/J.1365-2672.2011.05119.X>.
- [43] N.M.C. Olsen, E. Thiran, T. Hasler, T. Vanzielegem, G.N. Belibasakis, J. Mahillon, M.J. Loessner, M. Schmelcher, Synergistic removal of static and dynamic *Staphylococcus aureus* biofilms by combined treatment with a bacteriophage endolysin and a polysaccharide depolymerase, *Viruses* 10 (2018) 438, <https://doi.org/10.3390/V10080438>.
- [44] M. Fenton, R. Keary, O. McAuliffe, R.P. Ross, J. O'Mahony, A. Coffey, Bacteriophage-derived peptidase CHAP(K) eliminates and prevents staphylococcal biofilms, *Int. J. Microbiol.* 2013 (2013), <https://doi.org/10.1155/2013/625341>.